Z. Phys. C – Particles and Fields 38, 3–14 (1988)

Zeitschrift für Physik C Particles and Fields

Oxygen-induced reactions at 60 *A* GeV and 200 *A* GeV studied by calorimetry*

S.P. Sorensen

University of Tennessee, Knoxville, and Oak Ridge National Laboratory, Oak Ridge, USA

WA 80 Collaboration

R. Albrecht,[3] T.C. Awes,[2] C. Baktash,[2] P. Beckmann,[4] F. Berger,[4] R. Bock,[3] G. Claesson,[3] L. Dragon,[4] R.L. Ferguson,[2] A. Franz,[5] S. Garpmann,[6] R. Glasow,[4] H.A. Gustafsson,[6] H.H. Gutbrod,[3] K.H. Kampert,[4] B.W. Kolb,[3] P. Kristiansson,[5] I.Y. Lee,[2] H. Lohner,[4] I. Lund,[3] F.E. Obenshain,[1,2] A. Oskarsson,[6] I. Otterlund,[6] T. Peitzmann,[4] S. Persson,[6] F. Plasil,[2] A.M. Poskanzer,[5] M. Purschke,[4] H.G. Ritter,[5] R. Santo,[4] H.R. Schmidt,[3] T. Siemiarczuk,[3,a] S.P. Sorensen,[1,2] E. Stenlund,[6] G.R. Young[2]

[1] University of Tennessee, Knoxville, TN 37996, USA
[2] Oak Ridge National Laboratory, Oak Ridge, TN 37831, USA
[3] Gesellschaft für Schwerionenforschung (GSI), D-6100 Darmstadt, Federal Republic of Germany
[4] University of Münster, D-4400 Münster, Federal Republic of Germany
[5] Lawrence Berkeley Laboratory, Berkeley, CA 94720, USA
[6] University of Lund, S-22362 Lund, Sweden

Abstract. Results based on calorimetric measurements are presented from reactions of 60 *A* GeV and 200 *A* GeV ^{16}O projectiles with C, Cu, Ag, and Au nuclei. Minimum-bias cross sections are discussed. Energy spectra measured at zero degrees and transverse-energy distributions for the pseudorapidity range $2.4 \leqq \eta \leq 5.5$ are shown. An analysis of the average transverse energy in terms of the number of participating nucleons and the number of binary nucleon-nucleon collisions is presented. Estimates of nuclear stopping and of attained energy densities are made.

1 Introduction

The study of heavy ion collisions at ultrarelativistic energies is a new and exciting field on the borderline between nuclear and high energy physics. Presently, the primary goal is to verify the existence of the postulated quark-gluon plasma (QGP) [1]. A broad spectrum of possible plasma signatures has been suggested [1, 2]. An unfortunate common characteristic of most of these signatures is the necessity to distinguish them from the background created by nonplasma events. A thorough understanding of the reaction mechanisms in ultrarelativistic heavy ion collisions is, therefore, an important prerequisite in any QGP search. This paper presents some of the first steps taken in this direction by the WA 80 collaboration. The focus will be on data obtained with our calorimeters, with special emphasis on the results which can be extracted from forward calorimetry.

In an effort to isolate characteristic features of nucleus-nucleus collisions (e.g., collective phenomena) from those that may be expected on the basis of a linear superposition of nucleon-nucleon collisions, we will compare measured quantities with calculations that reproduce data from nucleon-induced reactions and that make predictions for nucleus-nucleus reactions. While several models are available for this procedure, none has yet been demonstrated to have clear advantages over the others. Consequently, we have chosen to make comparisons with the Lund model for high-energy nucleus-nucleus interactions (FRITIOF) [3]. Effects of detector acceptance and of trigger bias have been included in all FRITIOF simula-

* Presented at the 6th International Conference on Ultra-Relativistic Nucleus-Neucleus Collisions – Quark Matter 1987, 24–28 August 1987, Nordkirchen, Federal Republic of Germany

[a] On leave of absence from the Institute for Nuclear Studies, Warsaw, Poland

tions shown in this work except for the total reaction cross section calculations. In describing the nuclear density, the radius parameter $r_0 = 1.10$ fm has been used for the Woods-Saxon distributions. This results in somewhat larger sizes of the light nuclei as compared to the standard FRITIOF parameter selection but is in better agreement with results for the nuclear density distribution from electron scattering [4].

Another theme in our current analysis is the extraction of results from the data with minimal use of complicated models. Some reliance on models is, however, needed in any interpretation of experimental data. An analysis of the transverse energy generated in terms of the number of participating nucleons and the number of binary nucleon-nucleon collisions will be presented in Sect. 6. Although the extraction of these numbers is not model-independent, it is based primarily on simple geometrical aspects of the nuclear collisions.

Finally results on nuclear stopping and energy densities are presented in Sect. 7 and 8, respectively.

2 Experimental setup

The measurements described in this paper were performed with the WA 80 experimental arrangement [5, 6] at the CERN SPS. The setup includes two calorimeters: the Mid-Rapidity Calorimeter (MIRAC) and the Zero-Degree Calorimeter (ZDC) [7]. MIRAC consists of 30 stacks with each stack subdivided into six 20×20 cm^2 towers. Each tower consists of a lead/scintillator electromagnetic section of 15.6 radiation lengths (0.8 absorption lengths) and an iron/scintillator hadronic section of 6.1 absorption lengths. MIRAC is organized into five groups of six stacks, called six-packs, each with dimensions of 1.3×1.2 m^2. Four of the six-packs are arranged in a wall around the beam axis at a distance of 6.5 m from the target and with a 7.5×7.5 cm^2 hole in the center to allow the beam to reach the ZDC. The MIRAC wall has full azimuthal coverage in pseudorapidity, η, from 2.4 to 5.5 with partial coverage extending down to 2.0. The fifth six-pack of MIRAC is placed next to the MIRAC wall, where it covers approximately 10% of the azimuthal angles in the pseudorapidity interval from 1.6 to 2.4 The measured σ/E resolutions of the calorimeter are 14.2% for 10 GeV/c charged pions and 5.1% for 10 GeV/c electrons [7].

The ZDC is a 60×60 cm^2 uranium/scintillator calorimeter divided into an electromagnetic section of 20.5 radiation lengths and a hadronic section of 9.6 absorption lengths. The ZDC is located 11 m from the target and measures the energy of particles that pass through the beam hole in MIRAC. This hole has an inscribed cone angle of 0.3 deg, corresponding to $\eta > 6.0$. The ZDC is both a key component of the trigger system and an important measuring device from which the total energy of projectile spectators and/or of the leading particles is obtained. The resolution of the ZDC is 2.5% at 3.2 TeV and 4.5% at 0.96 TeV.

All data presented in this paper were obtained under the minimum-bias condition. This condition is defined by the requirements that: (*a*) less than 88% of the full projectile energy is measured by the ZDC and (*b*) at least one charged particle is recorded by the multiplicity arrays in the interval $1.3 < \eta < 4.4$.

3 Reaction cross sections

Usually the first quantities to be measured in a new field of nuclear physics are the reaction cross sections. We will not deviate from this practice and present in Table 1 the measured minimum-bias cross sections, together with two sets of FRITIOF calculations: the total reaction cross section based on the requirement that at least one nucleon from the projectile collides with a target nucleon, and the minimum-bias cross sections, based on simulated trigger constrains in the FRITIOF-generated events. Systematic errors on the absolute cross sections are estimated to be less than 10%. FRITIOF reproduces both the energy and the target dependence of the measured minimum-bias cross sections also to within 10%.

Table 1. Reaction cross sections. Systematic errors on the experimental cross sections are estimated to less than 10%. Please refer to the next for the definition of the minimum-bias condition. r_0 and b are fitted Bradt-Peters parameters

$E_{lab} = 60$ *A* GeV	min bias σ_{EXP} [mb]	min bias $\sigma_{FRITIOF}$ [mb]	reaction $\sigma_{FRITIOF}$ [mb]
$^{16}O + ^{12}C$	650	650	1100
$^{16}O + ^{65}Cu$	1650	1440	2100
$^{16}O + ^{108}Ag$	2250	1950	2630
$^{16}O + ^{197}Au$	2900	2660	3360
r_0 [fm]	1.46	1.32	1.26
b [fm]	−2.34	−1.82	−0.08

$E_{lab} = 200$ A GeV	min bias σ_{EXP} [mb]	min bias $\sigma_{FRITIOF}$ [mb]	reaction $\sigma_{FRITIOF}$ [mb]
$^{16}O + ^{12}C$	450	460	1100
$^{16}O + ^{65}Cu$	1350	1270	2100
$^{16}O + ^{108}Ag$	1800	1660	2630
$^{16}O + ^{197}Au$	2450	2290	3360
r_0 [fm]	1.44	1.41	1.26
b [fm]	−3.02	−2.92	−0.08

The target dependence is given approximately by the sum of the transverse areas of the nuclei as expressed in the Bradt-Peters parametrization [8]

$$\sigma = \pi r_0^2 (A_p^{1/3} + A_t^{1/3} + b)^2. \tag{1}$$

The radius parameter, r_0, and the overlap parameter b extracted from the A_t dependence of the cross sections are also shown in Table 1. It is noteworthy that the overlap parameter for the FRITIOF total reaction cross sections is practically zero, whereas the minimum-bias cross sections show a large negative value of b. This indicates that b is to a larger extent a measure of the trigger bias in this experiment than an estimate of the overlap between two nuclei in reactions where at least one nucleon-nucleon collision takes place.

While the calculated reaction cross sections show no energy dependence, the minimum-bias cross sections show a strong energy dependence. This dependence originates from different acceptances of the minimum-bias trigger at the two beam energies and can be understood from the following argument.

In a reaction with a given impact parameter the ratio between the energy deposited in the Zero-Degree Calorimeter, E_{ZDC}, and the beam energy, E_{beam}, can be expressed as

$$\frac{E_{ZDC}}{E_{beam}} = \frac{E_{Sp} + E_{reac}(\eta > 6)}{E_{Sp} + E_{reac}}, \tag{2}$$

where E_{Sp} is the energy carried by the projectile spectators, and E_{reac} is the reaction energy or, equivalently, the energy carried by the projectile participants, and $E_{reac}(\eta > 6)$ is the reaction energy accepted by the 0.3° beam hole in MIRAC. In going from 60 A GeV to 200 A GeV, the nucleon-nucleon CM rapidity increases from 2.4 to 3.0. As a consequence, if there is no significant change in the reaction mechanism, $E_{reac}(\eta > 6)$ will constitute a larger fraction of E_{reac} at the higher bombarding energy and E_{Sp} will, therefore, have to constitute a smaller fraction of E_{beam} in order to fulfill the most stringent of the trigger requirements, namely $E_{ZDC} < 0.88 * E_{beam}$. Smaller values of E_{Sp}/E_{beam} implie smaller impact parameters and, thereby, smaller total minimum-bias cross sections at the higher beam energy.

4 Zero-degree energy distributions

An important aspect of high energy nucleus-nucleus collisions is the nuclear collision geometry [9–11] as determined by the relative sizes of the target and projectile nuclei, the overlap volume in the collision, and the impact parameter. As a consequence, simple geometrical considerations can be used as a key for a qualitative understanding of the ZDC energy spectra shown as filled circles in Fig. 1. At 200 A GeV, the $^{16}O + ^{12}C$ reaction has essentially no cross section for events depositing a small amount of energy in the ZDC because, in a simple participant spectator picture, even in the most central collisions, several projectile spectator nucleons, each with an energy of 200 GeV, proceed in the beam direction. In contrast, a pronounced peak is seen at small ZDC energies in the spectrum from the $^{16}O + ^{197}Au$ reaction. In this case, events with low ZDC energies result from central collisions in which the oxygen projectile is engulfed by the massive Au nucleus, resulting in the emission of only a few leading particles at angles less than 0.3 deg. Furthermore, in this case, a wide range of impact parameters gives rise to collisions in which the entire projectile interacts with a nearly constant number of target nucleons, thus producing the peak at low ZDC energies.

The effects of the more restricted acceptance of the ZDC in going from 200 A GeV to 60 A GeV, as discussed above, is clearly seen in the 60 A GeV $^{16}O + ^{197}Au$ spectrum, which has an even more pronounced peak at the lowest energies. In the 60 A GeV $^{16}O + ^{12}C$ reaction there are many more events with low ZDC energies as compared to the 200 A GeV case. These events may originate from collisions in which the oxygen projectile fragments so violently that one or more of the projectile spectators has a pseudorapidity lower than 6 and is thereby intercepted by MIRAC.

The predictions of the FRITIOF model are shown as histograms in Fig. 1. The agreement with the data is generally better at 200 A GeV than at 60 A GeV. There is a clear tendency for FRITIOF to underestimate the cross section for small values of E_{ZDC}. This could indicate that FRITIOF does not include a sufficiently large degree of longitudinal momentum transfer in binary nucleon-nucleon collisions, but a final conclusion on this point will have to wait until the nuclear density prescription in FRITIOF has been further evaluated.

5 Transverse energy distributions

The transverse energy produced in the reaction is measured on an event-by-event basis in MIRAC. The transverse energy is calculated as $E_T = \Sigma E_i \sin(\theta_i)$, where E_i and θ_i are the observed energy and the effective angle of each element i of MIRAC, respectively. The estimated systematic error in the transverse energy scale is less than 10%. Based on measurements of the response of the calorimeter to electrons, pions, and protons of known energies between 2 and

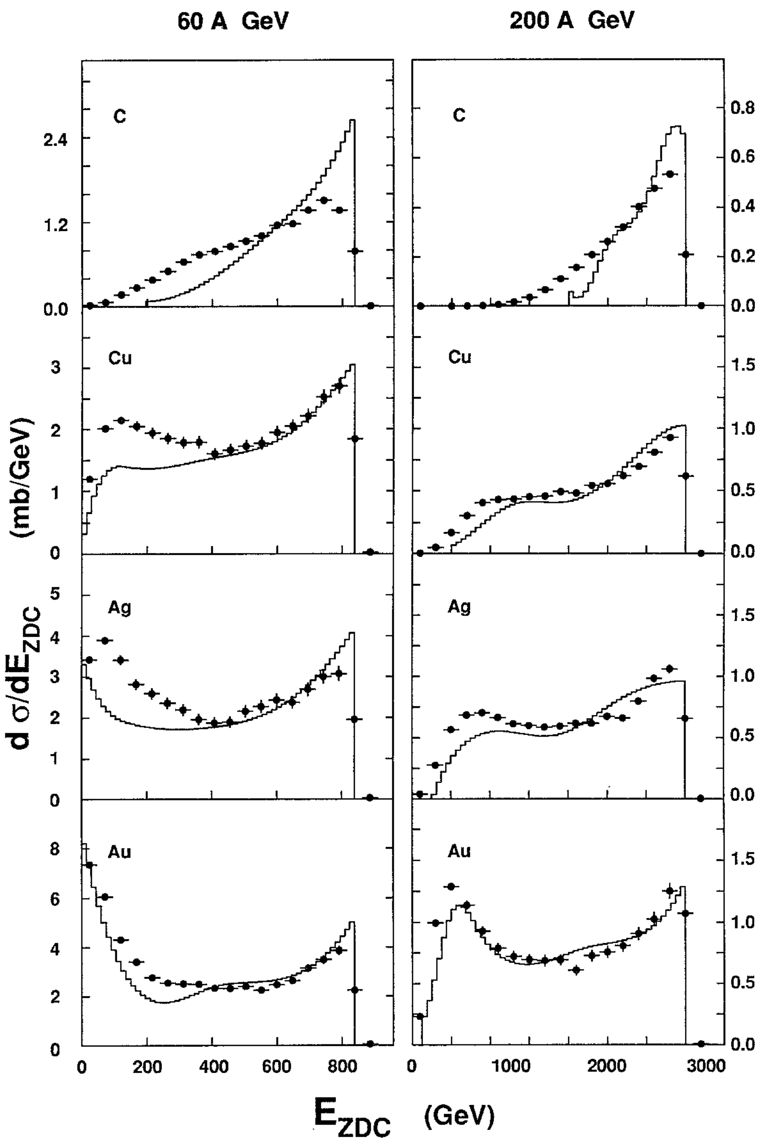

Fig. 1. Energy spectra measured in the Zero-Degree Calorimeter (filled circles) in ^{16}O induced reactions. Histograms give the results of the FRITIOF model [3]. The vertical error bars represent statistical errors

50 GeV, an iterative procedure has been developed by means of which the nonprojective features of the calorimeter response are corrected for. The method is described in detail elsewhere [7, 12].

The transverse energy distributions for $2.4<\eta<5.5$ are shown as filled circles in Fig. 2. As in the case of the ZDC spectra, the shapes of the E_T spectra are dominated by effects of the nuclear geometry. The spectra for the heaviest nuclei, Ag and Au, show a large "plateau" extending out to 80–100 GeV at 200 A GeV beam energy and to 40–45 GeV at 60 A GeV. The Au spectra have a broad peak at the high-energy end of the plateau. This peak is closely correlated with the low-energy peak in the Au ZDC spectra [9]. This correlation demonstrates that the peak in the E_T distribution, corresponding to low ZDC energies, originates from the most central collisions, in which the entire projectile interacts with a nearly constant number of target nucleons. As the target becomes smaller, the peak and the plateau become less pronounced. For $^{16}O+{}^{12}C$, the E_T spectra have shapes similar to those of the E_T spectra measured in proton-induced reactions [13], whereas the heavy target spectra are similar, both in shape and energy scale, to the E_T spectra for 200 A GeV ^{16}O +Pb of the NA 35 collaboration [10].

At 60 A GeV, the high-energy tails of the E_T distributions for Cu, Ag, and Au targets almost coincide with one another at a value of approximately 60 GeV. This phenomenon could be caused by "complete stopping" as discussed by the E802 collaboration for data obtained at 15 A GeV [14]. However, at our beam energies, this finding is more likely to be due to a combination of two opposing effects. As the target mass or number of target participants increases, the maximum transverse energy increases. At the

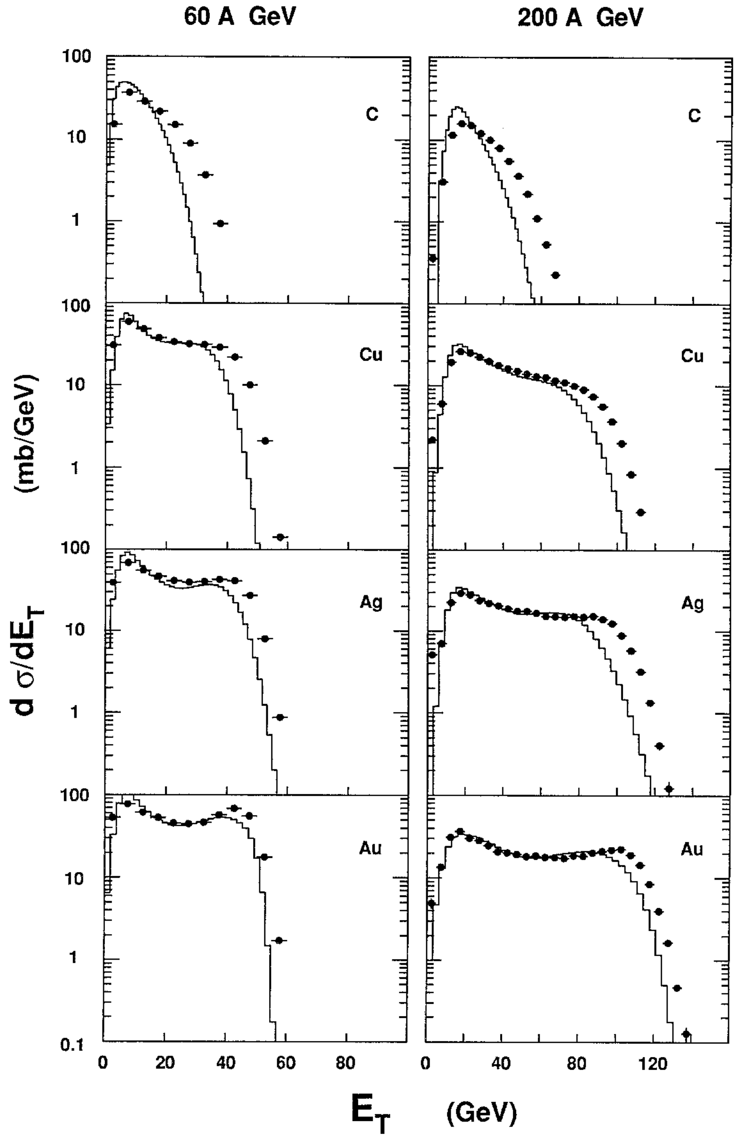

Fig. 2. Transverse energy distributions measured in the pseudorapidity range of $2.4<\eta<5.5$ for 60 A GeV and 200 A GeV ^{16}O projectiles incident on targets of C, Cu, Ag, and Au. The experimental results (filled circles) are presented with their statistical errors. Histograms give the results of the FRITIOF model

same time, however, the rapidity of the effective CM system decreases, leading to decreased coverage by MIRAC. At 60 A GeV these two effects tend to cancel each other; whereas, at 200 A GeV the increase in E_T dominates over the decreasing coverage, resulting in a net increase of the observed transverse energy. This demonstrates that the precise shapes of the observed E_T spectra are a sensitive function of the pseudorapidity region in which they are measured. Thus, in measurements with coverage of the lower pseudorapidity region, no peak has been seen at high E_T for heavy targets [11]. FRITIOF calculations are consistent with this observation.

The histograms in Fig. 2 are the results of FRITIOF calculations. For the three heaviest targets at both bombarding energies the model gives a good description of the shapes of the E_T spectra but consistently underestimates the transverse energy scale in the tail region by 10% to 15%. For the $^{16}O+^{12}C$ case the discrepancies between the model and the data are even larger.

6 Participants and binary collisions

In view of the importance of the nuclear collision geometry, it is desirable to develop a simple method by means of which the impact parameter, b, the number of participating nucleons, W, and the number of binary nucleon-nucleon collisions, ν, can be determined. An estimate of the number of projectile participants, W_p, could be obtained from the ZDC with the simple assumption that all of the observed ZDC energy is due to projectile spectators. Similarly, the number of target participants, W_t, could be estimated on the assumption that all target nucleons lying in the path of the projectile are participants. This rela-

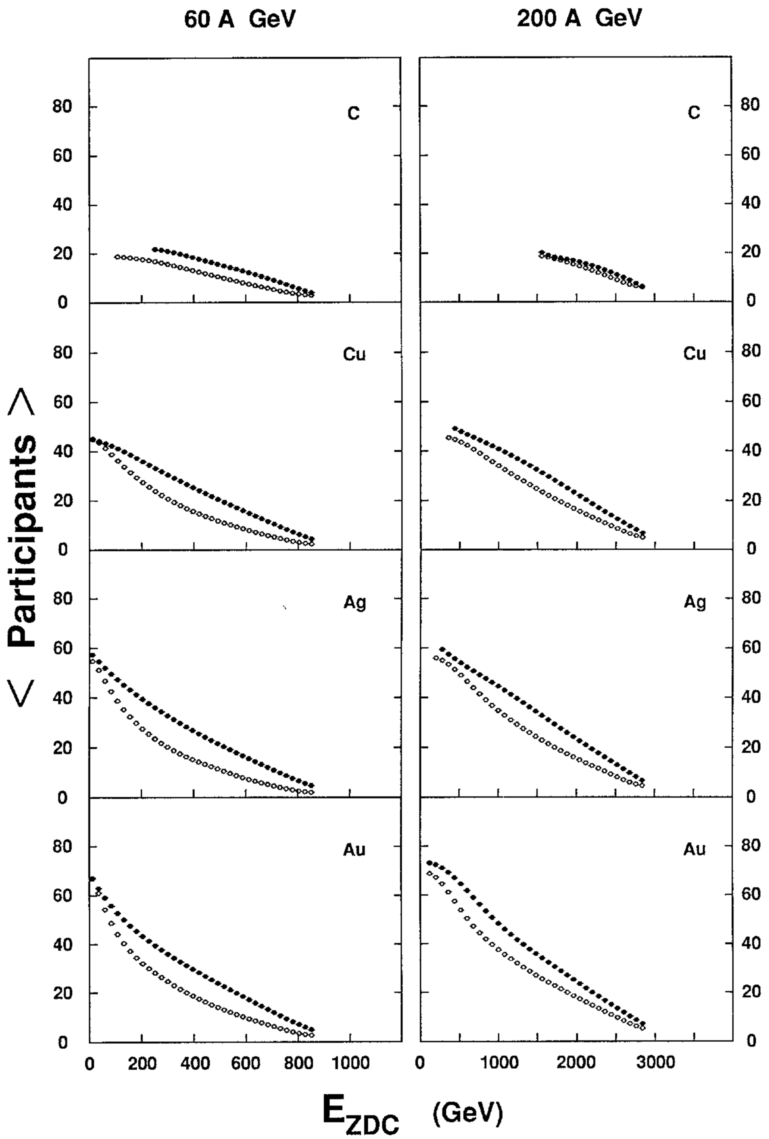

Fig. 3. The average number of participants as a function of the energy measured in the Zero-Degree Calorimeter. The filled circles indicate the results of FRITIOF calculations. The open circles give the results the slicing method (see text for details)

tionship between the ZDC energy and W_p is not, however, strictly valid in the presence of leading particles or of other reaction products with $\eta > 6.0$.

Therefore, two alternative methods have been used to obtain more accurate estimates of the average values of $\langle W \rangle$ and $\langle v \rangle$ for a given E_{ZDC}. It is important to emphasize that the analysis presented here investigates only the first moments of W and v. This implies that for all other quantities discussed in this section, e.g. E_T/W and E_T/v, only the behaviour averaged over a large sample of events is investigated and fluctuations are not considered.

In the first method, FRITIOF calculations have been used to establish the relationship between E_{ZDC} and both $\langle W \rangle$ and $\langle v \rangle$. The underlying assumption in this method is that FRITIOF is able to describe the ZDC spectra, which is not strictly the case. The results of this "calibration" of E_{ZDC} in terms of $\langle W \rangle$ and $\langle v \rangle$ are shown as filled circles in Fig. 3 and 4, respectively. These curves demonstrate the primary virtue of the Zero-Degree Calorimeter as a detector of the collision centrality: the lowest values of E_{ZDC} clearly correspond to the most central collisions with the largest values of $\langle W \rangle$ and $\langle v \rangle$.

The second method, denoted as the "slicing" method, is based on the assumption of a monotonic increase of E_{ZDC} as a function of the impact parameter. Due to fluctuations, both in the nuclear collision and in the detector response, this assumption is not strictly correct on an event-by-event basis. The validity of the method will, therefore, be determined by the relative size of the standard deviation of b for fixed values of E_{ZDC}, σ_b, and $\langle b \rangle$. Simulations indicate that σ_b is of the order of 0.5 fm for all values of E_{ZDC}. The formalism of the slicing method is outlined below.

For a given value of the energy deposited in the

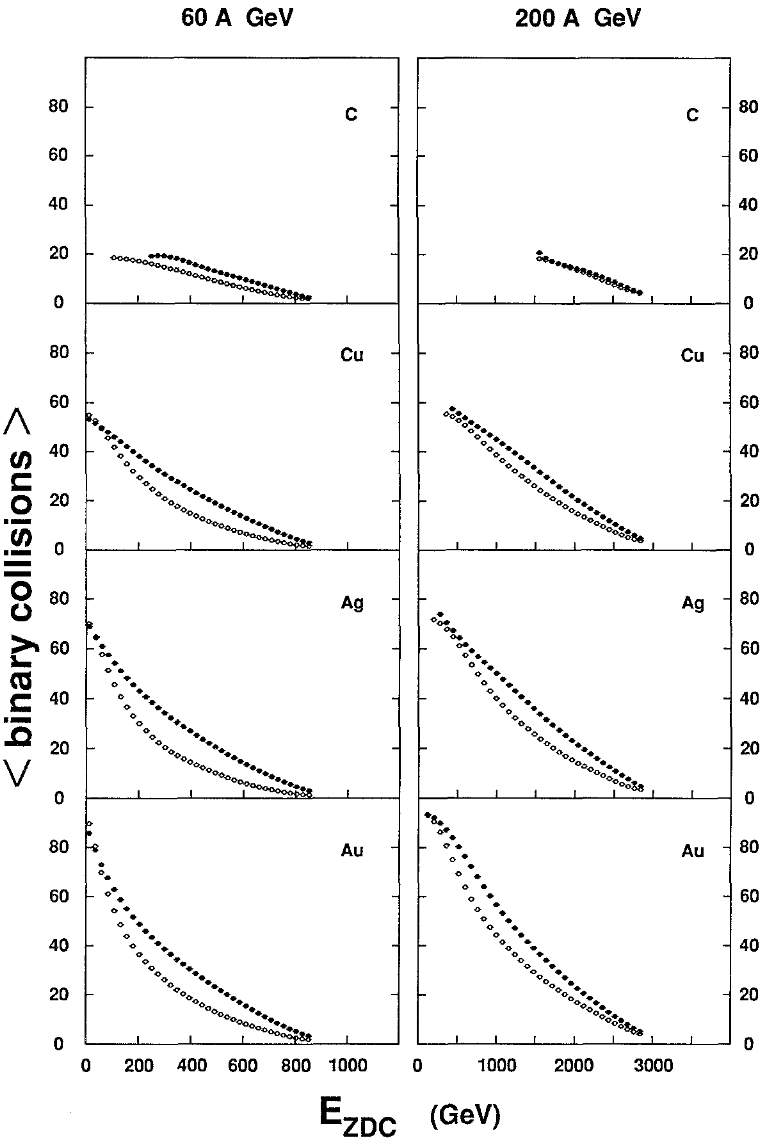

Fig. 4. The average number of binary nucleon-nucleon collisions as a function of the energy measured in the Zero-Degree Calorimeter. See Fig. 3 for the definitions of the symbols

ZDC, E^0_{ZDC}, the average impact parameter b is calculated from the relation:

$$\pi b^2 = \int_0^{E^0_{\mathrm{ZDC}}} \frac{d\sigma}{dE_{\mathrm{ZDC}}} dE_{\mathrm{ZCD}}. \tag{3}$$

Once b is known, $\langle W \rangle$ and $\langle \nu \rangle$ can be calculated using Glauber theory [15–17]. First, the thickness function, $T_t(\mathbf{b}_t)$, for the target is calculated at a transverse distance, $\mathbf{b}_t$, from its center:

$$T_t(\mathbf{b}_t) = \int \rho_t(\mathbf{b}_t, z)\, dz, \tag{4}$$

where the nucleon density ρ is normalized to unity

$$\int \rho_t(\mathbf{r})\, d\mathbf{r} = 1. \tag{5}$$

Identical formulae hold for the projectile and are denoted by the index p. For nuclei with $A > 16$, the nucleon density is given by a Woods-Saxon distribution with radius $R = 1.12\, A^{1/3} - 0.86\, A^{-1/3}$ fm and diffuseness $a = 0.54$ fm [4]. For lighter nuclei the parametrization [18]

$$\rho(r) = \rho(0)\left[1 + \alpha\left(\frac{r}{R}\right)^2\right] \exp\left[-\left(\frac{r}{R}\right)^2\right] \tag{6}$$

has been used with parameters (R, α) chosen as (1.71 fm, 1.12) and (1.82 fm, 1.60) for ^{12}C and ^{16}O, respectively.

The average number of participants from the target, W_t, is then given by

$$W_t = A_t \int d\mathbf{b}_t\, T_t(\mathbf{b}_t)\, [1 - [1 - T_p(\mathbf{b} + \mathbf{b}_t)\, \sigma_{nn}]^{A_p}], \tag{7}$$

where $\sigma_{nn} = 29.4$ mb [16] is the inelastic nucleon-nucleon cross section. The impact parameter vector, $\mathbf{b}$, is chosen as (0, b) for convenience. The average total

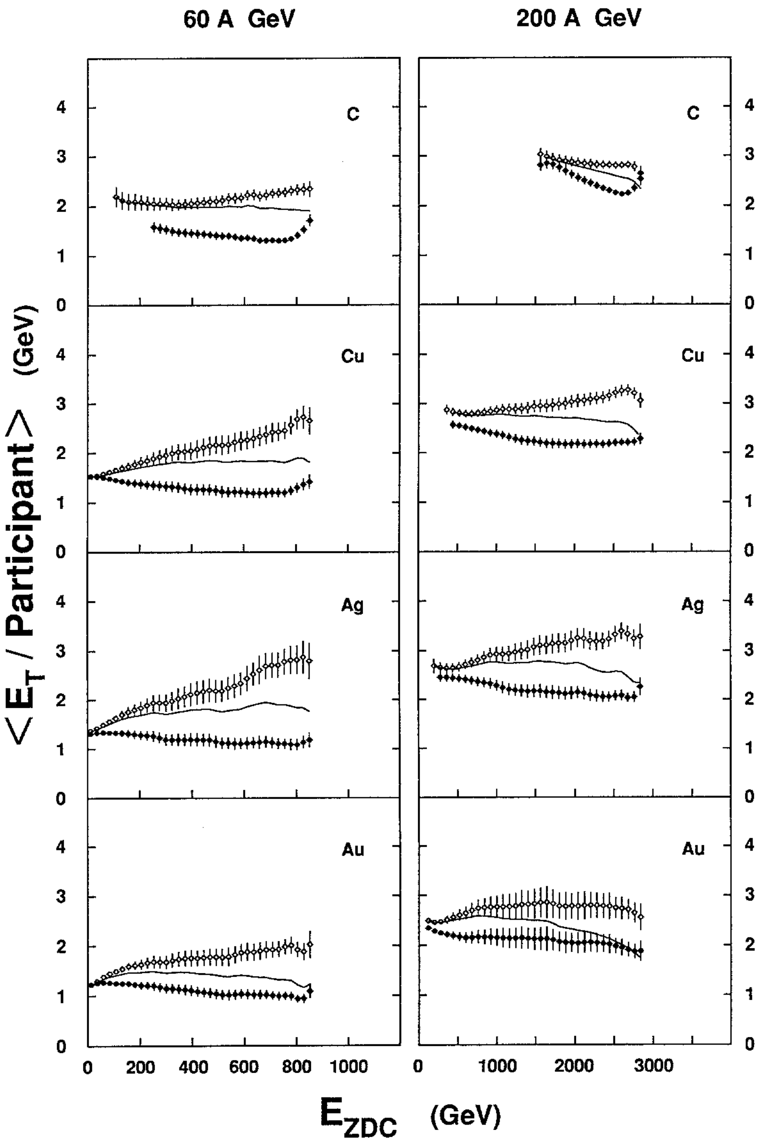

Fig. 5. Average values of E_T/participant as a function of the energy measured in the Zero-Degree Calorimeter. The pseudorapidity range used in the E_T determination is $1.6<\eta<5.5$. Open and filled circle definitions identical to Fig. 3. The solid curves are the results of the slicing method with 10% reduced absolute cross sections

number of participants is finally obtained from

$$W = W_t + W_p. \tag{8}$$

In order to extract $\langle \nu \rangle$, the nucleus-nucleus thickness function at the impact parameter b is calculated as

$$T(\mathbf{b}) = \int d\mathbf{b}_t\, T_p(\mathbf{b}+\mathbf{b}_t)\, T_t(\mathbf{b}_t). \tag{9}$$

The average number of binary collisions is then

$$\langle \nu \rangle (b) = T(b)\, \sigma_{nn}\, A_t\, A_p. \tag{10}$$

More complicated expressions can be derived for $\langle W \rangle$ and $\langle \nu \rangle$ in the case where the averages exclude those nuclear encounters in which there are not any binary collisions. For the impact parameters where the above formulae will be applied this probability is extremely small and can be neglected.

Combining (3) with (7) and (10) gives $\langle W \rangle$ and $\langle \nu \rangle$ as a function of E_{ZDC}. The results are shown as open circles in Figs. 3 and 4. The values obtained from FRITIOF are consistently larger than the values from the slicing method. This is due to two factors: 1) for a given impact parameter the Glauber theory gives somewhat smaller values of W and ν than FRITIOF and 2) the discrepancy between FRITIOF and $d\sigma/dE_{ZDC}$ at small values of E_{ZDC} results in larger values of b extracted from (3) for a given E_{ZDC} than predicted by FRITIOF.

The curves in Figs. 3 and 4 can now be utilized in many aspects of the data analysis. Here they will be used to investigate how the transverse energy depends on $\langle W \rangle$ and $\langle \nu \rangle$.

In Fig. 5, the average E_T per participant is shown as a function of E_{ZDC}. This $\langle E_T/W \rangle$ is calculated using the azimuthal-acceptance-corrected E_T measured

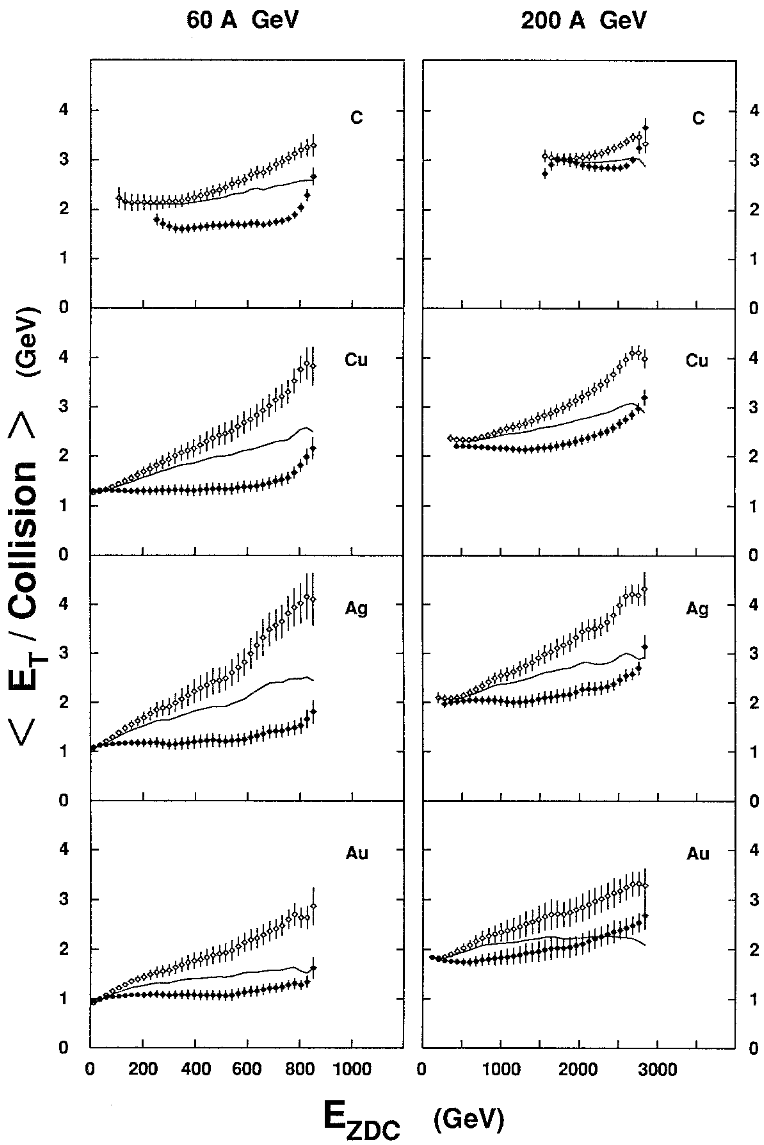

Fig. 6. Average values of E_T per binary nucleon-nucleon collision as a function of the energy measured in the Zero-Degree Calorimeter. The pseudorapidity range used in the E_T determination is $1.6<\eta<5.5$. See Fig. 5 for the definitions of the symbols

in the pseudorapidity interval $1.6<\eta<5.5$. The filled circles are based on the FRITIOF-calculated $\langle W \rangle$, and the open circles result from the slicing method. Similarly, the $\langle E_T/\nu \rangle$ is shown in Fig. 6.

The FRITIOF-based results clearly indicate that, on the average, the transverse energy is determined by the number of participating nucleons, with $\langle E_T/W \rangle$ increasing from 1.0–1.5 GeV at 60 A GeV to 2.0–2.5 at 200 A GeV. For the $\langle E_T/\nu \rangle$ the values are decreasing slightly with increasing centrality, as would be expected if the leading nucleon loses energy after each collision.

The values extracted from the slicing method are consistently larger than the FRITIOF-based values and do not show the same constancy of either $\langle E_T/W \rangle$ or $\langle E_T/\nu \rangle$. An important factor, however, in evaluating these results is the sensitivity of the slicing method to the absolute cross sections. The solid curves in Figs. 5 and 6 show the result of the slicing method, if the absolute cross section scale is lowered by only 10%, corresponding to the estimated maximum systematic error. The sensitivity of the slicing method to the absolute cross section is easily seen, especially for the most peripheral collisions. At the current stage in our analysis we are, therefore, inclined to put more emphasis on the results obtained from the FRITIOF-based method.

It should be noted, however, that for central collisions, where the geometry is well-defined and which from a QGP-search point of view is by far the most interesting, the two methods give nearly identical results. It is remarkable that in this case, $\langle E_T/W \rangle$ and $\langle E_T/\nu \rangle$ are approximately target-independent at a given bombarding energy.

7 Nuclear stopping

The degree of nuclear stopping is a key quantity in discussions of the probability of quark-gluon plasma formation. Due to difficulties associated with a precise definition of "nuclear stopping", our stopping results are presented in terms of two different ratios, S_{int} and S_{mid}, of the measured and theoretical values of transverse energies, evaluated in two different ways. The maximum value of the transverse energy, $E_T^{\max}$, can be estimated under the assumptions that: (*a*) in central collisions all the projectile nucleons react with a cylinder of the target nucleus that has a base area equal to the cross section of the projectile; and (*b*) all of the available center of mass energy, E'_{cm}, is emitted isotropically in the CM system. E'_{cm} is obtained from the CM energy by subtracting the rest mass of the participating baryons. In this simple model $E_T^{\max} = \pi/4 * E'_{\text{cm}}$ and $[dE_T(\text{theory})/d\eta]_{\max} = E'_{\text{cm}}/2$. Numerical details of the calculation are indicated in Table 2. In the analysis of the experimental data, only central events have been considered by restricting the number of participants to be larger than 24, 45, 50, and 55 for C, Cu, Ag, and Au, respectively. By fitting the experimental $dE_T/d\eta$ distribution in the interval $1.6 < \eta < 5.5$ with a Gaussian distribution, the $E_T^{\text{integrated}}$ has been calculated as the integral of the fitted distribution. Likewise, the quantity $[dE_T(\text{experiment})/d\eta]_{\max}$ has been taken to be the maximum value of the Gaussian. The "integrated energy stopping", S_{int}, is defined as the ratio between $E_T^{\text{integrated}}$ and $E_T^{\max}$. This ratio is seen from Table 2 to decrease from 57% at 60 *A* GeV to 51% at 200 *A* GeV for $^{16}O + ^{197}Au$.

Probably a more relevant number for the stopping is the "mid-rapidity energy stopping", S_{mid}, defined as the ratio between $[dE_T(\text{experiment})/d\eta]_{\max}$ and $[dE_T(\text{theory})/d\eta]_{\max}$. The systematics of this quantity are shown in Table 3. At 60 *A* GeV S_{mid} is about 1/3 and only decreasing to 1/4 at 200 *A* GeV. S_{mid} appears to be only very weakly dependent on the target mass.

It should be stressed that, in the above dicussions of nuclear stopping, the isotropic source model has only been introduced to estimate the largest possible kinematical limits. Other models will result in larger values of the stopping. In this connection it is interesting to note that the model of Rafelski and Schnabel [19] leads to values very close to 100% for *both* S_{int} and S_{mid} at *both* bombarding energies for O + Au.

Table 2. Calculation of the "integrated energy stopping" and the "mid-rapidity energy stopping" in central collisions of $^{16}O + ^{197}Au$

E_{beam}	60 *A* GeV	200 *A* GeV
N^t_{part} (number of target participants)	52.0	52.0
E_{cm} (GeV)	309.2	559.1
$E'_{\text{cm}} = E_{\text{cm}} - (M^{\text{proj}} + M^t_{\text{part}})c^2$ (GeV)	245.8	495.7
$E_T^{\max} = \pi/4 * E'_{\text{cm}}$ (GeV)	193.1	389.4
$[dE_T(\text{theory})/d\eta]_{\max} = E'_{\text{cm}}/2$ (GeV)	122.9	247.9
$E_T^{\text{integrated}}$ (GeV)	109 (16)	197 (30)
$[dE_T(\text{experiment})/d\eta]_{\max}$ (GeV)	43 (5)	66 (7)
$S_{\text{int}} = E_T^{\text{integrated}}/E_T^{\max}$	57 (9)%	51 (8)%
$S_{\text{mid}} = \dfrac{[dE_T(\text{experiment})/d\eta]_{\max}}{[dE_T(\text{theory})/d\eta]_{\max}}$	35 (4)%	27 (3)%

Table 3. "Mid-rapidity energy stopping" for ^{16}O + C, Cu, Ag, and Au at 60 *A* GeV and 200 *A* GeV

	60 *A* GeV	200 *A* GeV
C	31 (3)%	21 (2)%
Cu	32 (3)%	26 (3)%
Ag	35 (4)%	26 (3)%
Au	35 (4)%	27 (3)%

8 Energy densities

At present, no generally accepted method exists for the determination of the energy density, ε, from experimental results. We estimate ε from the following formula, which is based on the work of Bjorken [20] and Kajantie and McLerran [21]

$$\varepsilon = \frac{1}{\tau_0 \pi R^2} \frac{dE_T}{dy}. \tag{11}$$

Here τ_0 was taken to be 1 fm/c, and the sharp-surface electron-scattering value of 3.0 fm was used for R, the radius of ^{16}O [18]. Rapidity was replaced by pseudorapidity, and an interval of $2.4 < \eta < 4.0$ was used. Values of ε obtained by this prescription are believed to be underestimates of true energy densities attained [2], unless a larger value of $\tau_0 = 2$ fm/c is used, as indicated by Ranft [22]. The tail of the ε distribution calculated from (11) extends to 1.3 GeV/fm^3 at 60 *A* GeV and as high as 2.7 GeV/fm^3 at 200 A GeV, reaching, in this case, the region of energy densities that are believed to be required for the formation of the quark-gluon plasma. The value of ε at 200 *A* GeV is similar to an energy density of 2.2 GeV/fm^3 for average central collisions as measured by the NA 35 collaboration [10].

Glauber calculations, as discussed in Sect. 6, show that the average number of participants in the most central O + Au, S + Au and Pb + Pb collisions will be 70, 115, and 390, respectively. Since the transverse energy generated in central collisions seems to scale approximately with the number of participants, the maximum E_T in S+Au and Pb+Pb collisions will be 1.7 and 5.7 times larger than for O+Au. However, the ratios of the transverse areas of the projectiles scales as $(32/16)^{2/3}=1.6$ and $(208/16)^{2/3}=5.5$, indicating that the *volume-averaged* energy densities will not increase by using larger projectiles. The gain will be in the larger volume of the high energy density matter and the larger central energy density, as the following discussion demonstrates.

For central collisions at 200 A GeV our data show that $[dE_T/d\eta]_{\max}$ scales approximately with the number of participants, W, with a factor of proportionality close to 0.9 GeV/nucleon

$$\frac{d^2 E_T}{d\eta\, dW}=0.9 \text{ GeV/nucleon (central collisions).}$$

Along the symmetry axis in a central collision the total number of participants per unit transverse area will be

$$\left.\frac{dW}{dA_\perp}\right]_{R=0}=2\rho_0\, r_0 (A_p^{1/3}+A_t^{1/3}). \tag{12}$$

The central energy density $\varepsilon_{\text{central}}$ will, therefore, approximately be given as

$$\begin{aligned}\varepsilon_{\text{central}} &= \frac{1}{\tau_0}\frac{d^2 E_T}{d\eta\, dW}\left.\frac{dW}{dA_\perp}\right]_{R=0}\\ &=0.9\,\frac{2\rho_0\, r_0}{\tau_0}(A_p^{1/3}+A_t^{1/3})\\ &=0.35(A_p^{1/3}+A_t^{1/3})\,[\text{GeV/fm}^3],\end{aligned} \tag{13}$$

where the following numerical values have been used: $\rho_0=0.16\ \text{fm}^{-3}$, $r_0=1.20$ fm and $\tau_0=1$ fm/c. Equation [13] shows that the gain in going to larger projectiles will be in the central energy density, which will increase as $A_p^{1/3}$. The attainable values of $\varepsilon_{\text{central}}$ in average central collisions at 200 A GeV for some much discussed systems are:

O +Au: 2.9 GeV/fm^3
S +Au: 3.1 GeV/fm^3
Pb+Pb: 4.1 GeV/fm^3
U +U: 4.8 GeV/fm^3 (tip-on-tip collision).

The absolute numerical values shown here will, of course, scale with the inverse of the formation time τ_0 and should, therefore, be viewed with caution. The large value of $\varepsilon_{\text{central}}$ for a tip-on-tip U+U central collision suggests that consideration should be given to Uranium beams in plans for future upgrades of ultrarelativistic heavy-ion accelerator facilities.

9 Conclusions

In summary, results have been presented from reactions of 60 A GeV and 200 A GeV ^{16}O projectiles with various target nuclei. Minimum-bias cross sections, energy measurements for $\eta>6.0$, and E_T distributions for $2.4<\eta<5.5$ were shown. The importance of the collision geometry was stressed and used to extract the average total participant number and the average number of binary nucleon-nucleon collisions as functions of the energy deposited in the Zero-Degree Calorimeter. These extracted numbers were in turn used to show that the average transverse energy per participant is approximately independent of target mass at a given bombarding energy. Estimates of the nuclear stopping showed only a small decrease with increasing bombarding energy. Based on the Bjorken formula, the volume-averaged energy densities in central O+Au collisions reach up to 2.7 GeV/fm^3. Estimates of the central energy densities were made, showing that this quantity will scale as $A_p^{1/3}$, whereas the energy density averaged over the total reaction volume will probably only show a very weak projectile dependence.

Acknowledgements. We appreciate the excellent work of the accelerator divisions of CERN, GSI, and LBL, which has resulted in the development and delivery of the oxygen beams used in this work. Valuable discussions with C.Y. Wong on the slicing method are gratefully acknowledged. Partial support by the West German BMFT and DFG, the United States DOE, the Swedish NFR, the Humboldt Foundation and the CERN-EP Division is gratefully acknowledged.

References

1. See, for example, T. Ludlam, H. Wegner: Nucl. Phys. A418 (1984); Proc. Fourth Int. Conf. on Ultrarelativistic Nucleus-Nucleus Collisions, Helsinki, Finland, 1984, K. Kajantie (ed.). Lecture Notes in Physics 221, Berlin, Heidelberg, New York: Springer 1984; L.S. Schroeder, M. Gyulassy: Nucl. Phys. **A461** (1987); L. McLerran: Rev. Mod. Phys. **58** (1986) 1021 and references therein
2. L. van Hove: Proc. Second Int. Conf. on Nucleus-Nucleus Collisions, Visby, Sweden, 1985; H.-A. Gustafsson, B. Jakobsson, I. Otterlund, K. Aleklett (eds.) Amsterdam: North-Holland, 1986
3. B. Nilsson-Almqvist, E. Stenlund: Comp. Phys. Commun. **43** (1987) 387; B. Andersson et al.: Phys. Rep. 97 (1983) 31; B. Andersson et al.: Phys. Scr. 34 (1986) 451; B. Andersson et al.: Lund University Report LU-TP 86-3, Lund, Sweden (1986)
4. A. Bohr, B. Mottelson: Nuclear Structure, Vol. I. New York: A. Benjamin 1969
5. WA 80 Collab. R. Albrecht et al.: Report No. GSI-85-32, Gesellschaft für Schwerionenforschung, D-6100 Darmstadt, W. Germany (1985)
6. WA 80 Collab. H.H. Gutbrod et al.: Proc. Int. Workshop on Gross Properties of Nuclei and Nuclear Excitations XV, Hirschegg, Austria, 1987, Hans Feldmeier (ed.) Darmstadt Report ISSN 0720-8715, p. 42 (1987)
7. T.C. Awes et al.: to be submitted to Nucl. Instrum. Methods

8. H.L. Bradt, B. Peters: Phys. Rev. 77 (1950) 54; P.J. Karol: Phys. Rev. C11 (1975) 1203; H.H. Heckman et al.: Phys. Rev. C17 (1978) 1735
9. WA 80 Collab. R. Albrecht et al.: accepted for publication in Phys. Lett. B
10. NA 35 Collab. A. Bamberger et al.: Phys. Lett. 184B (1987) 271
11. NA 34 Collab. T. Akesson et al.: to be published in Z. Phys. C – Particles and Fields
12. WA 80 Collab. S.P. Sorensen: Nucl. Phys. A461 (1987) 487c
13. A. Franz: The transverse energy flow in hadron-lead collisions at 200 GeV/*c* incoming momentum, Ph. D. thesis, University of Siegen (1986); T. Akesson et al.: Nucl. Phys. A447 (1985) 475c; R. Gomez et al.: Phys. Rev. D35 (1987) 2736
14. E 802 Collab. T. Abbott et al.: to be published in Phys. Lett. B
15. R.J. Glauber: In: Lectures in theoretical physics, Vol. 1, 315. W.E. Brittin, L.G. Durham (eds.) New York: Interscience 1959
16. C.-Y. Wong: Phys. Rev. D30 (1984) 972; C.-Y. Wong: Phys. Rev. D32 (1985) 94
17. S. Date et al.: Phys. Rev. D32 (1985) 619
18. H.F. Ehrenberg et al.: Phys. Rev. 113 (1959) 666
19. J. Rafelski, A. Schnabel: Univ. of Cape Town, preprint, UCT-TP 81/1987
20. J.D. Bjorken: Phys. Rev. D27 (1983) 140
21. K. Kajantie, L. McLerran: Univ. of Helsinki preprint, HU-TFT-82-30, 1982
22. J. Ranft: preprint, SSC-143, 1987 (submitted to Phys. Rev. D)